

SolarSLAM: Battery-free Loop Closure for Indoor Localisation

Bo Wei^{1*}, Weitao Xu², Chengwen Luo³, Guillaume Zoppi⁴, Dong Ma⁵, Sen Wang⁶

Abstract—In this paper, we propose SolarSLAM, a battery-free loop closure method for indoor localisation. Inertial Measurement Unit (IMU) based indoor localisation method has been widely used due to its ubiquity in mobile devices, such as mobile phones, smartwatches and wearable bands. However, it suffers from the unavoidable long term drift. To mitigate the localisation error, many loop closure solutions have been proposed using sophisticated sensors, such as cameras, laser, etc. Despite achieving high-precision localisation performance, these sensors consume a huge amount of energy. Different from those solutions, the proposed SolarSLAM takes advantage of an energy harvesting solar cell as a sensor and achieves effective battery-free loop closure method. The proposed method suggests the key-point dynamic time warping for detecting loops and uses robust simultaneous localisation and mapping (SLAM) as the optimiser to remove falsely recognised loop closures. Extensive evaluations in the real environments have been conducted to demonstrate the advantageous photocurrent characteristics for indoor localisation and good localisation accuracy of the proposed method.

Index Terms—Indoor localisation, SLAM, Solar cell

I. INTRODUCTION

The proliferation of wearable devices and wireless technologies in the last decade has resulted in a wide range of mobile and ubiquitous services, including indoor localisation. Indoor localisation has a huge potential for many application scenarios, e.g. navigation in office areas, shopping malls, and museums. However, despite significant research progress, developing an efficient and practical indoor localisation system remains a challenge.

Since the Global Positioning System (GPS) fails to offer accurate localisation information without good reception of its signal in an indoor environment, various indoor localisation systems have been developed in the past decades

This research was funded by the Engineering and Physical Sciences Research Council (EPSRC) Robotics and Artificial Intelligence ORCA Hub (Grant EP/R026173/1), EPSRC North East Centre for Energy Materials (NECEM, Grant EP/R021503/1) and EU H2020 Programme under Deep-Field project (ID 857339).

¹ Bo Wei is with Department of Computer and Information Sciences, Northumbria University, Newcastle upon Tyne, United Kingdom. bo.wei@northumbria.ac.uk (* Corresponding author).

² Weitao Xu is with Department of Computer Science, City University of Hong Kong, Hong Kong, China weitaoxu@cityu.edu.hk

³ Chengwen Luo is with College of Computer Science and Software Engineering, Shenzhen University, Shenzhen, China chengwen@szu.edu.cn

⁴ Guillaume Zoppi is with Department of Mathematics, Physics and Electrical Engineering, Northumbria University, Newcastle upon Tyne, United Kingdom guillaume.zoppi@northumbria.ac.uk

⁵ Dong Ma is with Department of Computer Science and Technology, University of Cambridge, Cambridge, United Kingdom dm878@cam.ac.uk

⁶ Sen Wang is with School of Engineering & Physical Sciences, Heriot-Watt University, Edinburgh, United Kingdom s.wang@hw.ac.uk

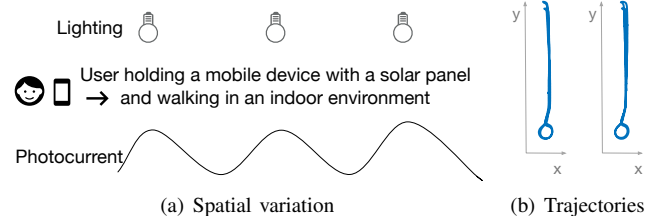


Fig. 1. Feasibility Study (a) Spatial variation (b) Ground truth trajectory (left) and recovered trajectory (right)

[1]–[3]. Among the solutions, Inertial Measurement Unit (IMU) based pedestrian dead reckoning (PDR) is a promising technique due to the ubiquity of IMUs in mobile devices. By using this method, only one IMU is carried by the user to localise itself. However, the localisation drift always occurs caused by the inevitable IMU sensor bias. Therefore, extra sensors are usually required for data fusion, which corrects the errors generated from the IMU sensor and provides accurate localisation performance. Popular data fusion methods for mobile devices are camera based [1], WiFi based [2], Ultra-wide Band (UWB) based [3], etc. These sensors can be used for fusing with inertial data, which significantly improves the IMU based localisation performance and provides fairly good accuracy in the indoor environment. However, those sensors cost a massive amount of energy, which limits their long term use in mobile devices. Extensive research has been conducted towards improving localisation accuracy, but limited attention has been paid to reduce the energy consumption of an indoor localisation system.

In this paper, we present a battery-free loop closure method for indoor localisation system, which is named SolarSLAM. The key feature of SolarSLAM is the use of an off-the-shelf solar cell. The advantage of the use of solar cells over existing sensors is the capability of energy harvesting and photocurrent generation even with indoor illumination [4]. Furthermore, the amplitude of its generated photocurrent is extremely sensitive to different lighting conditions, while the lighting condition in one particular position usually does not change in the indoor environment. Motivated by these facts, we use one solar cell along with an IMU for indoor localisation. The stability of the spot-wise indoor lighting condition and the sensitivity of solar cell generated photocurrent due to varying lighting conditions offer the feasibility of the use of a solar cell to close loops for indoor localisation when the user revisits one place.

The use of solar cells, though has not been widely studied in wearable devices at the moment, is a promising future battery-free solution for various mobile applications such as activity recognition [5], gesture recognition [6], [7] etc.

Different from the existing applications, we are the first to use one solar cell as a sensor for closing loops in an indoor localisation application. In the near future, we can envision that solar panel-based energy harvesting can be integrated into wearable devices [8]. Thus, our solution can take advantage of this technique to achieve battery-free indoor localisation. Even though the lighting condition in an indoor environment is usually not as optimistic as that under direct sunshine on sunny days, it still can generate a certain level of photocurrent. When a portion of a solar panel is covered or the lighting condition changes, its output photocurrent will change accordingly. In an indoor environment, the variation of the lighting condition along one path follows the identical pattern. When one user revisits one area, the solar cell can capture the same lighting variance from its generated photocurrent and indicate the user's returning one location. The photocurrent measurements from revisits can be taken advantage for loop closures and calibrating the biased IMU based PDR trajectory estimate. Evaluation results show that the proposed method increases localisation performance up to 80% compared with the IMU based method. The solar cell, as a sensor, is capable of offering high-precision signals without consuming any energy, which can provide the support of long term execution of indoor localisation.

To summarise, the contributions of this paper are as follows:

- We are the first to use solar cells for indoor localisation because of their stability and sensitivity of indoor lighting conditions. A key-component dynamic time warping (DTW) has been proposed to find loop closures and improve the matching robustness.
- We implement an indoor localisation system, which conducts data fusion between inertial measurements and photocurrent from a solar cell.
- Extensive experiments have been conducted to evaluate our proposed localisation methods in the real environments.

In the rest part of this paper, Section II shows the related works. Section III overviews the system. Our proposed battery-free loop closure methods for indoor localisation will be shown in detail in Section IV. In Section V, we conduct extensive experiments in real environments and evaluate our proposed methods to show its feasibility, efficacy and robustness.

II. RELATED WORKS

Many localisation methods have been based on various sensors, such as camera [1] and laser [9]. They can achieve high-precision accuracy in ideal conditions, but they cost extremely high energy, which makes them infeasible for the long term use by mobile devices with limited energy. WiFi signal is widely available in indoor environments, such as office building, shopping mall, etc. Therefore, WiFi based indoor localisation systems have been well studied [2], [10]. The recent wireless communication standard IEEE 802.11mc has integrated the ranging and localisation into WiFi standard

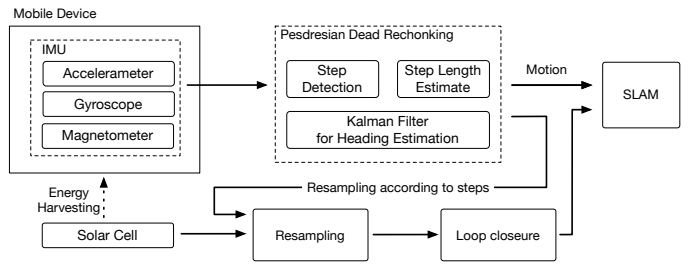


Fig. 2. System overview of the battery-free loop closure method for indoor localisation

[11], and the latest Android phones have started to support this protocol [12]. However, WiFi based localisation would require to install several access points to achieve reasonable accuracy. The localisation performance of these systems is also affected by multipath effect [13]. UWB is a promising indoor localisation technique, which is able to offer high precision centimetre-level accuracy [14]. Roetenberg et al. fused UWB signal with inertial measurements and designed a context awareness system [3]. To achieve good accuracy, it requires a proper transmitter geometry placed in the periphery of an Area of Interest with a good line-of-sight. Magnetic induction devices were also used with IMU and achieved accurate and robust indoor localisation [15].

Recently, researchers have taken advantage of solar cells as sensors to convert the generated photocurrent to the usable spatial and temporal information for many context awareness applications. Randall et al. [5] used the wearable solar cells to track the changing lighting for localisation and activity recognition. The light emitter model was analysed and used to estimate the distance between the solar cells and the known lights. Different from this work, our method does not need any prior knowledge and the location information of the lighting source. Chen et al. [16] used the solar energy information and exposed the locations of the solar-powered home with the assumption of anonymity, which achieved the accuracy within 20km. Umetsu et al. [17] explored solar cells along with random forest machine learning techniques for place recognition. The implemented system was able to distinguish 10 places under different weather and time periods. Varshney et al. [7] designed a visible light sensing system for communication and context awareness, which enabled recognition for 3 gestures. Ma et al. [6] used a transparent solar panel to conduct gesture recognition and achieved the 96% accuracy, and the designed system saved more than 40% power compared to the use of a photodiode.

III. SYSTEM OVERVIEW

Figure 2 shows an overview of the proposed system. The proposed indoor localisation system consists of two sensors, i.e. a motion sensor IMU and a solar cell. The IMU continuously provides motion measurements using a PDR method. In our system, we use a handheld mobile phone with the integration of an IMU and apply the robust PDR method to obtain the initial trajectory estimate from the integrated accelerometer, gyroscope and magnetometer. In the robust PDR, step detection mechanism has been utilised to mitigate

the bias from hardware design. However, suffering from biased measurements, the indoor localisation using an IMU still fails to achieve a satisfactory localisation performance. One popular calibration method is loop closure to indicate the user revisits one same place, where one auxiliary sensor is usually required to calibrate the bias.

In this paper, we propose to use a solar cell as a sensor to close loops. Along with motion measurements from an IMU, the generated photocurrent from the solar cell is measured simultaneously, which reflects the dynamic lighting condition in different locations. DTW has been explored to determine the user's revisiting. Our proposed loop closure methods have addressed several challenges, such as time unsynchronisation and changing walking speed, etc. Simultaneous localisation and mapping (SLAM) has been used as the optimiser to fuse inertial measurements and photocurrent measurements.

The details of the proposed system will be described in Section IV.

IV. METHOD

In this section, we will show the technical details of SLAM, robust PDR, and the proposed loop closure method.

A. SLAM Framework

We show the explored SLAM framework in detail in this section. In the proposed architecture, our system uses a robust GraphSLAM optimiser [18], [19]. The original GraphSLAM optimiser [20], [21] considers all the constraints from odometry and loop closures with equal weights, as shown in Equation 1.

$$\operatorname{argmin}_Y \sum_{i \in S} u_i^T \Lambda_i u_i \quad (1)$$

where Y is the estimated trajectory, S is the constraint set, u and Λ are error terms and information matrix for the relevant constraint. The constraint set includes both motion and loop closure constraints with equal weightings. However, the use of photocurrent from the solar cells for loop closure generates many false positives. Figure 3(a) shows the similarity of the collected photocurrent measurements along one corridor, where the intermediate distance between each pair of lights are the same. This is very common in the indoor environment. The similarity of the light deployment will generate false matches because it is difficult to ascertain the differences among these similar instances.

To avoid false matching, we use robust SLAM in our system. Different from the original SLAM, the optimal trajectory Y^* will be derived using the following optimiser instead [19],

$$\operatorname{argmin}_Y \underbrace{\sum_{i \in C_O} u_i^T \Lambda_i u_i}_{(C1)} + \underbrace{\sum_{i \in C_L} \alpha_i^2 u_i^T \Lambda_i u_i}_{(C2)} \quad (2)$$

The robust SLAM also considers constraints from two sources as demonstrated in Equation 2, i.e. (C1) motion constraints from the IMU trajectory and (C2) loop closures from the solar cell, respectively. u and Λ also represent the error terms and information matrix in Equation 2. To remove the outliers and enable a strong optimiser, the robust SLAM

adds scaling factors α for each information matrix of the loop closure constraints. Equation 3 shows the calculation of the scaling factor α_i ,

$$\alpha_i = \min\left(1, \frac{2\Gamma}{\Gamma + K_i^2}\right) \quad (3)$$

where $K_i = u_i^T \alpha_i u_i$ is for i -th photocurrent loop closure constraint from Equation 2 and Γ is a free parameter. The use of the scaling factor α during the optimisation can significantly and effectively reduce the impact of false-positive loop closures, which removes false matching from photocurrent. More information can be found in [19].

B. Robust PDR

Our proposed method employs a robust PDR method¹ [22]. Using PDR and the ubiquity of IMU, a mobile device is able to offer the user's motion without relying on any other sensors. As shown in Figure 2, PDR has three key components, i.e., step detection, step length estimation and heading estimation. Acceleration measurements are used for calculating the step length with the use of Weinberg algorithm [23] and step detection with a threshold of signal amplitude. Heading estimation is gauged from gyroscope measurements and magnetometer measurements. The PDR can derive the step length L_s as the displacement and the relative orientation θ as the heading change with respect to the previous pose for each step. The use of a robust PDR can tremendously reduce the localisation error for the movement of each step, but it still suffers from the unavoidable long term drift. Figure 5(g) shows the trajectory using PDR in one experiment, and the trajectory is drifted over a long period of time compared with the ground truth in Figure 5(f). To overcome this issue, the proposed method used battery-free solar cells as a sensor, detect loop closures and correct the long-term PDR drift.

C. Loop Closure Method

In this section, we will show the details of our proposed loop closure method using photocurrent measurements from solar cells.

1) *Photocurrent Measurement Resampling*: We use a solar cell as a sensor to collect the photocurrent measurements. Because the photocurrent is an analogue signal, it is collected from an analogue-to-digital converter (ADC) to convert analogue signals to digital signals. To synchronise photocurrent measurement with IMU measurements, the first task is to resample the photocurrent measurements before using them.

An efficient resampling method has been used in our system [24]. Here we introduce the details of the resampling method. The original signals S_o has the sampling rates (Hz) R_o . Our aim is to resample S_o from R_o to R_d . To realise this, $R_d - 1$ samples are interpolated into each pair of samples in S_o samples to create an intermediate signal S_m . One low-pass filter is then used to S_i to avoid aliasing, and the filtered signal is denoted as \widehat{S}_m . Every R_d sample from the intermediate signal \widehat{S}_m is selected to obtain the resultant S_d .

¹The PDR code can be downloaded from <https://lopsie.weebly.com/teaching.html>

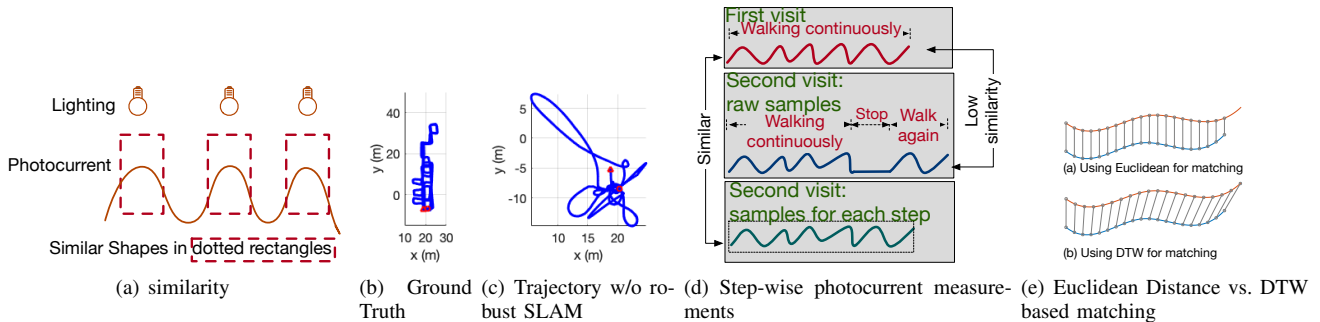


Fig. 3. Explanation: (a) Example of similarity of the collected photocurrent measurements along one corridor; (b) and (c) are the ground truth and the trajectory without the use of robust SLAM; (d) Measurements for revisiting one place; (e) The difference between Euclidean distance and DTW

The photocurrent measurements change with the lighting condition continuously, which provides the feasibility of interpolation and resampling without violating the usable patterns. In our system, photocurrent measurements are first resampled to the same sampling rate as the inertial measurements using the discussed resampling method. Then, the step-wise photocurrent measurements will be selected according to the step detection in the PDR algorithm from IMU measurements. Figure 3(d) shows one user revisits the same area but stops for a period of time. Without the use of the step-wise photocurrent measurements, the two instances cannot match and create a loop closure constraint. On the contrast, the removal of the temporal stopping points and the selection of photocurrent measurements for each step make the two instances virtually matching. Now we are ready to introduce the instance matching method.

2) *Principle Element Dynamic Time Warping for Effective Loop Closure* : When using DTW, the window size can affect the performance significantly. When using the original sampling rate, it is difficult to match two instances because the user may stop moving for a certain period of time, but the solar cells still continue to sense the lighting condition. To resolve this problem, we use the principle elements of the resampled photocurrent measurements with the assistant of an IMU. As introduced earlier, we use each step as a key point to select the step-wise photocurrent measurements for loop closure. Dynamic Time Warping (DTW) [25] is explored for matching two photocurrent measurement instances. DTW is a technique to measure the similarity of two time series of signals using dynamic programming. Figure 3(e) shows the difference between using Euclidean distance and DTW for matching. When using a Euclidean distance based method for matching two time-series signals, it calculates the distance between corresponding elements. By contrast, DTW considers phase misalignment. This is very important because of varying walking patterns and speed for our application scenario, which helps realise robust and effective loop closure detection using photocurrent measurements. A DTW distance threshold is set to determine the approximation of two instances.

V. EVALUATIONS

In this section, we will conduct evaluations to (1) show the feasibility of accurate loop closure and indoor localisation using photocurrent measurements; (2) present the localisation

performance in two indoor environments with people walking in the surrounding environment. The lighting condition does not change significantly in these indoor environments.

A. Hardware

Figure 4(a) shows the hardware for collecting photocurrent measurements. In the experiment, we use an off-the-shelf 1V solar cell to collect the photocurrent measurements. The solar cell is attached to the ADC in an mbed FRDM k64f [26] with the sampling rate 75Hz. The mbed FRDM k64f transfers the collected data to one laptop through a USB serial. The inertial measurements are recorded from an iPhone using the SensorLog App [27].

B. Feasibility Study

We will investigate the feasibility of the use of solar cell for indoor localisation and other context awareness applications in three aspects: stability, sensitivity and sequence similarity.

1) *Stability*: In this experiment, we put the solar cell in one spot and collect the data for approximately 8 minutes. Figure 4(b) shows the stability of the solar cell. The signal strength stays the same when the solar cell stays one position.

2) *Sensitivity*: The photocurrent signal is very sensitive to the position changes. To verify this, we put the solar cell on each corner of one piece of A4 paper with the size 21.0 cm \times 29.7 cm (shown in Figure 4(c)), where the length is much shorter than one step length (approximately 70 cm). It clearly demonstrates the differences among the photocurrent measurements in those four positions in Figure 4(d). The sensitivity, along with the discussed stability, provides unique spatial features and thus the feasibility of indoor localisation using photocurrent measurements.

3) *Sequence Similarity*: Figure 5(a) shows photocurrent measurements for 5 visits of the same path, i.e. a corridor. We can make a number of observations: (1) When looking at a sequence of photocurrent samples from that the monitored person walking in one corridor, the patterns of the photocurrent measurements in 5 visits are similar along the whole path and distinguishable in different spots. This fact makes the loop closure feasible when revisiting a location. (2) During collecting the data, the user tried to maintain the same speed, but the measurements are still not exactly the same. Therefore, DTW is more suitable with the proposed loop closure systems, which makes the proposed

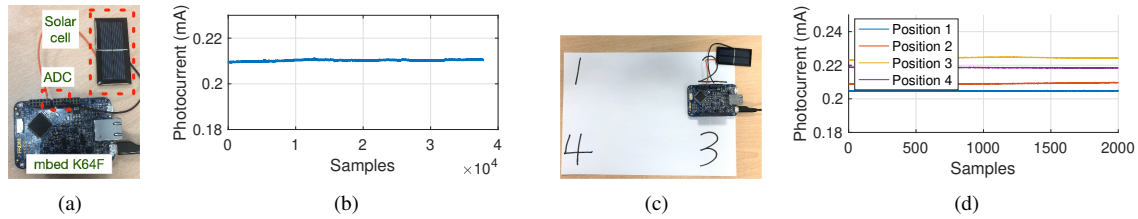


Fig. 4. (a) Hardware for collecting photocurrent measurements; (b) Stability of photocurrent measurements; (c) Solar cell put in each corner of a piece of A4 paper. In the figure, the solar cell is on the position 2; (d) Sensitivity of photocurrent measurements

localisation methods robust and effective. (3) Figure 5(a) demonstrates a number of examples of correct loop closures, which constructs constraint for the SLAM optimisation. (4) Several examples of false loop closures are also marked in Figure 5(a), which necessitates the robust SLAM as introduced in Section IV.

C. Experiments in an Office Building

In this section, we show the performance of the proposed SolarSLAM and compare it with the IMU based PDR. The goal of this experiment is to localise the monitored person who carries the solar cell and IMU and illustrate the efficiency of the loop closure methods. We consider 2D localisation in the experiments.

The following three metrics are used in this experiment: (1) Trajectory: the trajectories are able to show the localisation performance intuitively ; (2) *Root Mean Square Error (RMSE)*(e_{rms}): e_{rms} shows the average localisation error over the whole trajectory. $e_{rms} = \sqrt{\sum_{t=t_b}^{t_e} e(t)^2 / (t_e - t_b)}$, where $e(t)$ represents the localisation error with respect to time t . (3) *Cumulative distribution function (CDF) of tracking errors*: The CDF of tracking errors shows the frequency that a corresponding estimate error is less than or equal to the argument of that error.

The experiment area is $60 \text{ m} \times 5 \text{ m}$, and the trajectory path is 250.8 m. Figure 5(b) and Figure 5(c) show the ground truth and the trajectory of the IMU based PDR in the experiment. Figure 5(c) confirms that the IMU along with the robust PDR can localise the user in a certain level, but the IMU based PDR slowly drifts over time. Figure 5(d) shows the trajectory after using the proposed SolarSLAM method, which has corrected the IMU PDR localisation drift and is virtually indistinguishable as the ground truth. This has confirmed that the SolarSLAM has an excellent discriminative ability for loop-closure.

The e_{RMS} of IMU and the proposed SolarSLAM methods are 2.0733 m and 1.2498 m, respectively. Using the proposed SolarSLAM and fusing measurement from the solar cell and IMU, it can achieve 39.72% improvement compared with the IMU based PDR localisation method. Figure 5(e) shows the tracking CDF of errors using IMU based PDR and the proposed SolarSLAM method. The 80th percentile localisation errors for the IMU based PDR and the proposed SolarSLAM are 2.666 m and 1.526 m, respectively. In this metric, the proposed method achieves 45.76% improvement compared with the IMU based PDR.

D. Experiments in an Open Space Lab

The experiment is conducted in open space lab with desks, chairs, and computers. The lights in the cell are mostly evenly distributed, which caused excessive similarity of lighting conditions. The similarity of the lighting condition could result in a huge amount of falsely detected loop closures, which poses more challenges to the solar cell based indoor localisation. The carrier randomly walks in the $30 \text{ m} \times 60 \text{ m}$ areas, which leads the trajectory path 381.7 m. In this experiment, we use the same metrics in Section V-C to evaluate the performance of the proposed method.

Figure 5(f) and Figure 5(g) show the ground truth and the trajectory of the IMU based PDR in the experiment. Figure 5(g) shows the severe drifts of IMU based PDR over time. The proposed method corrects the IMU PDR localisation drift, as shown in Figure 5(h). The e_{RMS} of IMU and the proposed SolarSLAM methods are 10.7843 m and 1.8692 m, respectively. Using the proposed SolarSLAM and Fusing measurement from the solar cell and IMU, the proposed can achieve 82.67% improvements compared with the IMU based PDR localisation method. Figure 5(i) shows the tracking CDF of errors using IMU based PDR and the proposed SolarSLAM method. The 80th percentile localisation errors for the IMU based PDR and the proposed SolarSLAM are 15.31 m and 2.507 m, respectively. In this metric, the proposed method achieves 83.63% improvements compared with the IMU based PDR.

VI. CONCLUSION

In this paper, we propose the first system that uses a solar cell as a sensor for battery-free loop closure detection. An indoor localisation system has been implemented using a solar cell and IMU. The proposed loop closure method has corrected drift error from IMU error using robust SLAM method. Extensive experiments have been conducted to show the feasibility of one solar cell as a sensor for indoor localisation and context awareness. Our experiments in the real environment show that the use of the proposed method has increased the indoor localisation performance up to 80%.

REFERENCES

- [1] E. S. Jones and S. Soatto, "Visual-inertial navigation, mapping and localization: A scalable real-time causal approach," *The International Journal of Robotics Research*, jan 2011. [Online]. Available: <http://ijr.sagepub.com/cgi/doi/10.1177/0278364910388963>
- [2] J. Huang, D. Millman, M. Quigley, D. Stavens, S. Thrun, and A. Agarwal, "Efficient, generalized indoor WiFi GraphSLAM," *Proceedings - IEEE International Conference on Robotics and Automation*, pp. 1038–1043, 2011.

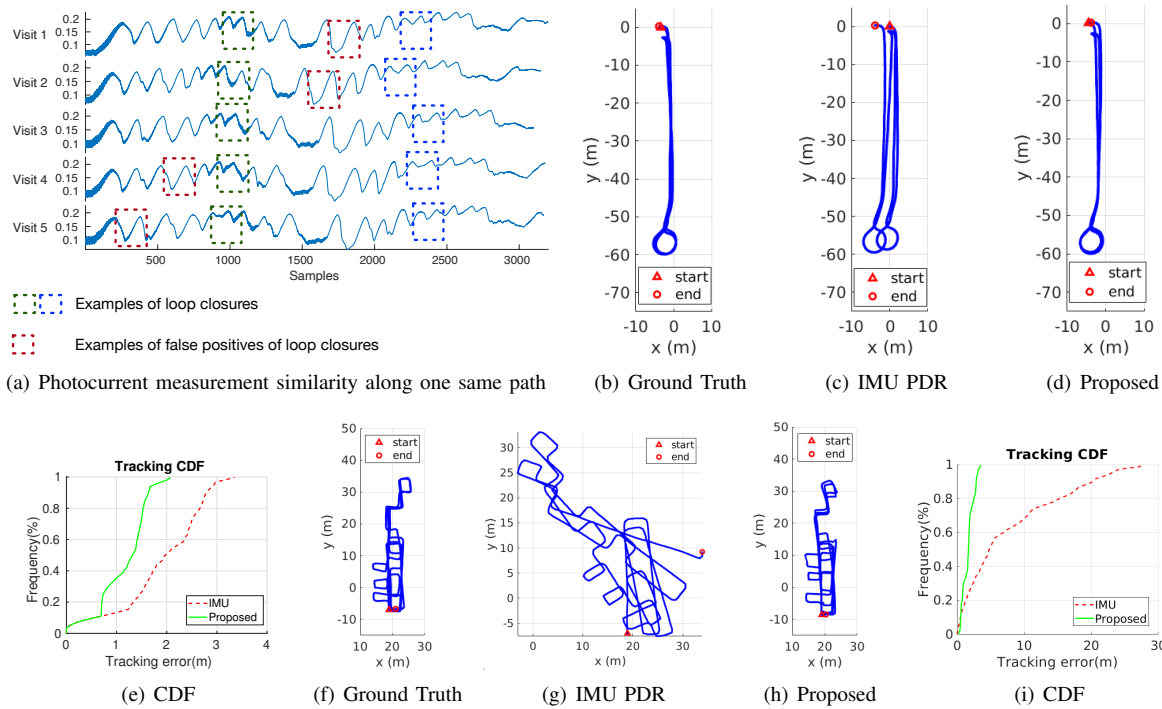


Fig. 5. Performances: (a) Photocurrent measurement similarity along one same path; (b)-(e) the performance of experiments in an office building; (f)-(i) the performance of experiments in an open space lab

[3] D. Roetenberg, H. Luinge, and P. Slycke, "Xsens mvn: full 6dof human motion tracking using miniature inertial sensors," *Xsens Motion Technologies BV, Tech. Rep.*, 2009.

[4] F. De Rossi, T. Pontecorvo, and T. M. Brown, "Characterization of photovoltaic devices for indoor light harvesting and customization of flexible dye solar cells to deliver superior efficiency under artificial lighting," *Applied Energy*, vol. 156, pp. 413–422, 2015.

[5] J. Randall, O. Amft, J. Bohn, and M. Burri, "Luxtrace: indoor positioning using building illumination," *Personal and ubiquitous computing*, vol. 11, no. 6, pp. 417–428, 2007.

[6] D. Ma, G. Lan, M. Hassan, W. Hu, M. B. Upama, A. Uddin, and M. Youssef, "Solargest: Ubiquitous and battery-free gesture recognition using solar cells," in *The 25th Annual International Conference on Mobile Computing and Networking*, ser. MobiCom '19. New York, NY, USA: Association for Computing Machinery, 2019. [Online]. Available: <https://doi.org/10.1145/3300061.3300129>

[7] A. Varshney, A. Soleiman, L. Mottola, and T. Voigt, "Battery-free visible light sensing," in *Proceedings of the 4th ACM Workshop on Visible Light Communication Systems*. ACM, 2017, pp. 3–8.

[8] Garmin and G. Ltd., "Garmin fenix 6x pro solar: Multisport gps watch." [Online]. Available: <https://buy.garmin.com/en-GB/GB/p/641375>

[9] "A Laser-Aided Inertial Navigation System (L-INS) for human localization in unknown indoor environments," *Proceedings - IEEE International Conference on Robotics and Automation*, pp. 5376–5382, 2010.

[10] B. Ferris, D. Fox, and N. Lawrence, "WiFi-SLAM using Gaussian process latent variable models," pp. 2480–2485, 2007.

[11] "Ieee 802.11tm wireless local area networks." [Online]. Available: <http://www.ieee802.org/11/>

[12] "Wi-fi rtt (ieee 802.11mc): Android open source project." [Online]. Available: <https://source.android.com/devices/tech/connect/wifi-rtt>

[13] B. Wei, A. Varshney, N. Patwari, W. Hu, T. Voigt, and C. T. Chou, "drti: Directional radio tomographic imaging," in *Proceedings of the 14th International Conference on Information Processing in Sensor Networks*. ACM, 2015, pp. 166–177.

[14] "Dacawave TREK1000 Evaluation Kit," <https://www.decawave.com/product/trek1000-evaluation-kit/>, accessed: 2019-10-23.

[15] B. Wei, N. Trigoni, and A. Markham, "imag: Accurate and rapidly deployable inertial magneto-inductive localisation," in *2018 IEEE International Conference on Robotics and Automation (ICRA)*. IEEE, 2018, pp. 99–106.

[16] D. Chen, S. Iyengar, D. Irwin, and P. Shenoy, "Sunspot: Exposing the location of anonymous solar-powered homes," in *Proceedings of the 3rd ACM International Conference on Systems for Energy-Efficient Built Environments*. ACM, 2016, pp. 85–94.

[17] Y. Umetsu, Y. Nakamura, Y. Arakawa, M. Fujimoto, and H. Suwa, "Ehaas: Energy harvesters as a sensor for place recognition on wearables," *2019 IEEE International Conference on Pervasive Computing and Communications (PerCom)*, pp. 1–10, 2019.

[18] R. Kummerle, G. Grisetti, H. Strasdat, K. Konolige, and W. Burgard, "G2o: A general framework for graph optimization," in *2011 IEEE International Conference on Robotics and Automation*. IEEE, may 2011, pp. 3607–3613. [Online]. Available: <http://ieeexplore.ieee.org/lpdocs/epic03/wrapper.htm?arnumber=5979949>

[19] P. Agarwal, G. D. Tipaldi, L. Spinello, C. Stachniss, and W. Burgard, "Robust map optimization using dynamic covariance scaling," in *2013 IEEE International Conference on Robotics and Automation*. Citeseer, 2013, pp. 62–69.

[20] S. Thrun and M. Montemerlo, "The GraphSLAM algorithm with applications to large-scale mapping of urban structures," *International Journal on Robotics Research*, vol. 25, no. 5/6, pp. 403–430, 2005.

[21] G. Grisetti, R. Kümmerle, C. Stachniss, U. Frese, and C. Hertzberg, "Hierarchical optimization on manifolds for online 2d and 3d mapping," in *2010 IEEE International Conference on Robotics and Automation*. IEEE, 2010, pp. 273–278.

[22] "Tutorials: Ipin 2017 pedestrian dead-reckoning (pdr) tutorial." [Online]. Available: <http://www.ipin2017.org/tutorials.html>

[23] H. Weinberg, "Using the adxl202 in pedometer and personal navigation applications," *Analog Devices AN-602 application note*, vol. 2, no. 2, pp. 1–6, 2002.

[24] K. Rajamani, Y.-S. Lai, and C. Furrow, "An efficient algorithm for sample rate conversion from cd to dat," *IEEE Signal Processing Letters*, vol. 7, no. 10, pp. 288–290, 2000.

[25] D. J. Berndt and J. Clifford, "Using dynamic time warping to find patterns in time series," in *KDD workshop*, vol. 10, no. 16. Seattle, WA, 1994, pp. 359–370.

[26] "mbed frdm k64f," <https://os.mbed.com/platforms/FRDM-K64F/>, accessed: 2020-01-09.

[27] "Sensorlog," <https://apps.apple.com/gb/app/sensorlog/id388014573>, accessed: 2020-01-09.